AIP | Review of Scientific Instruments

Note: Comparison between a prism-based and an acousto-optic tunable filter-based spectrometer for diffusive media

A. Farina, I. Bargigia, P. Taroni, and A. Pifferi

Citation: Review of Scientific Instruments **84**, 016109 (2013); doi: 10.1063/1.4789312
View online: http://dx.doi.org/10.1063/1.4789312
View Table of Contents: http://scitation.aip.org/content/aip/journal/rsi/84/1?ver=pdfcov
Published by the AIP Publishing

Note: Comparison between a prism-based and an acousto-optic tunable filter-based spectrometer for diffusive media

A. Farina,[1,a)] I. Bargigia,[2] P. Taroni,[1] and A. Pifferi[1,2]
[1]*Consiglio Nazionale delle Ricerche, Istituto di Fotonica e Nanotecnologie, Piazza L. da Vinci 32, I-20133 Milano, Italy*
[2]*Politecnico di Milano, Dipartimento di Fisica, Piazza L. Da Vinci 32, I-20133 Milano, Italy*

(Received 22 August 2012; accepted 9 January 2013; published online 23 January 2013)

This paper compares two continuously tunable systems for time-resolved spectroscopy of diffusive media based on a supercontinuum laser source. Two approaches for spectral selection are considered relying either on a dispersive prism or on a commercial acoustic-optic tunable filter (AOTF) device. The comparison was performed first in terms of extracted power and spectral response function, then in terms of distortions introduced in the retrieved absorption and scattering spectra. Simulations and experiments on diffusive phantoms confirmed that, besides narrower FWHM in the AOTF bandpass, the prism solution is superior with respect to the distortions produced on the recovered spectra.
 [http://dx.doi.org/10.1063/1.4789312]

Diffuse optical spectroscopy (DOS) is a fundamental tool for the characterization of a variety of highly diffusive media such as biological tissues,[1] fruits,[2] pharmaceutical tablets,[3] and wood.[4] Several approaches have been proposed for DOS: steady-state (SS),[5] time-resolved (TR),[6–9] and frequency-domain combined with SS.[10] Among these, TR offers a high sensitivity and the capability to retrieve separately absorption and reduced scattering coefficients from a single measurement of the distribution of photon times-of-flight (TOFs) detected at some point on the surface of the sample. Systems for broadband time-resolved spectroscopy (TRS) require laser sources tunable over a wide spectral range (typically 600–1100 nm for biological tissues) providing pulses on the picoseconds scale. The recent development of fiber lasers based on the generation of supercontinuum (SC) radiation in photonic-crystal fibers has opened the possibility to develop compact TRS systems suitable for the clinical environment.[11] These systems are usually coupled to an AOTF for wavelength selection purposes. Notwithstanding AOTF devices are largely used in diffuse optical spectroscopy,[2,9,12,13] their effects on the retrieved spectra have never been investigated. In fact, due to the long path length experienced by photons in highly diffusive media, absorption spectra can be strongly distorted by the non-ideal spectral response function (SRF) of the device used as a spectral filter.[14] In this work, we compare the effect of a commercial AOTF, usually sold together with a SC source, with a spectral filter based on a dispersive prism in a TRS system based on a SC pulsed laser and monochannel detection. The comparison is also supported by simulations.

The layout of the setup is shown in Fig. 1. The light source consists of a fiber laser (NKT Photonics, Denmark) providing white-light pulses shorter than 10 ps at a repetition rate of 80 MHz in the 450–1750 nm range with a total power of 5 W. The laser beam is expanded by means of a couple of achromatic doublets (Thorlabs, Germany) to reduce the beam divergence. Light is then dispersed by a SF10-glass Pellin-Broca prism (Bernhard Halle Nachfl.GmbH) and then focused on an adjustable slit (Thorlabs, Germany) for spectral width regulation. An image of the slit is then made on a 100 μm diameter graded-index fiber (Newport). Tuning is obtained by rotating the prism. The power at the sample can be adjusted by means of a motorized circular neutral-density filter placed in front of the fiber. A compact spectrometer (Ocean Optics) is used to monitor the SRF of the system. Light diffusely reflected by the sample is collected by a 1 mm diameter step-index fiber (Thorlabs, Germany) and then coupled to a microchannel plate (MCP) photomultiplier with S1 cathode (Hamamatsu, Japan). The acquisition of the temporal distribution of photon TOF is provided by a time-correlated single photon counting(TCSPC) board (Becker & Hickl, Germany) mounted on a computer. The acquisition is fully automated and controlled by home-made software. The temporal instrumental response function (IRF) of the system, including the temporal dispersion due to the fibers, is about 100 ps (FWHM). For the comparison, the dashed section in Fig. 1 is replaced by an AOTF (range 650–1100 nm) connected to a RF synthesizer (NKT Photonics, Denmark). The RF power values which guarantee the best side-lobes rejection have been saved by the manufacturer in the device memory. In the following, SYS1 stands for the prism-based system and SYS2 for the AOTF-based one.

In Fig. 2, peak-normalized SRFs of both systems are plotted for selected wavelengths. It is worth noting the presence of side-lobes in the SRF of SYS2. It is possible to observe that the power is, on average, higher for SYS1. This is due to the fact that the AOTF is polarization-dependent and one half of the total power is lost. Moreover, the efficiency of the AOTF decreases at the edge of the working spectral range. On the contrary, the prism can be tuned over the entire emission range of the source. The bandpass (FWHM) of SYS1 is broader for longer wavelengths due to the prism dispersion. This can be a drawback if one needs a high resolution spectral sampling, but it can also be an advantage because it compensates for the

a)Author to whom correspondence should be addressed. Electronic mail: andrea.farina@polimi.it.

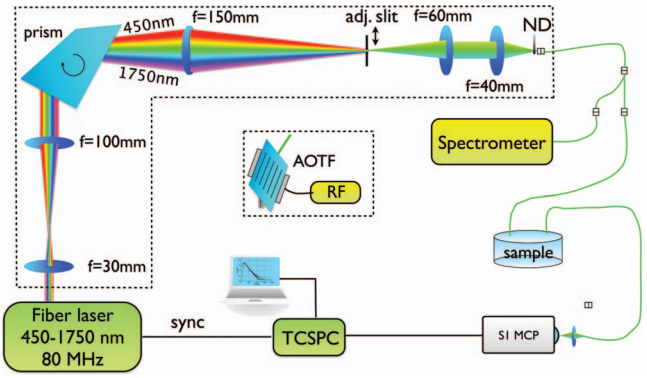

FIG. 1. TRS system. SYS1 is referred to the prism-based systems. SYS2 is obtained by substituting the dashed part of SYS1 with the dashed block in the center.

efficiency fall off of most detectors used in 600–1100 nm. On the other hand, the bandpass of SYS2 is on average narrower than for SYS1.

The effect of the SRF in TRS has been investigated first by means of simulations and then by an experimental measurement. For the simulations, time-resolved reflectance curves (2 cm source-detector separation) have been generated at different wavelengths under the diffusion approximation[15] for a semi-infinite medium at two constant reduced scattering coefficients ($\mu'_s = 5$ and 10 cm^{-1}), using the absorption spectrum of the water peak at 970 nm. These curves have then been summed together weighting each of them first with a gaussian function and then with a sinc^2 profile having both the same FWHM at each nominal wavelength. These functions represent a typical SRF of a prism- and AOTF-based system,

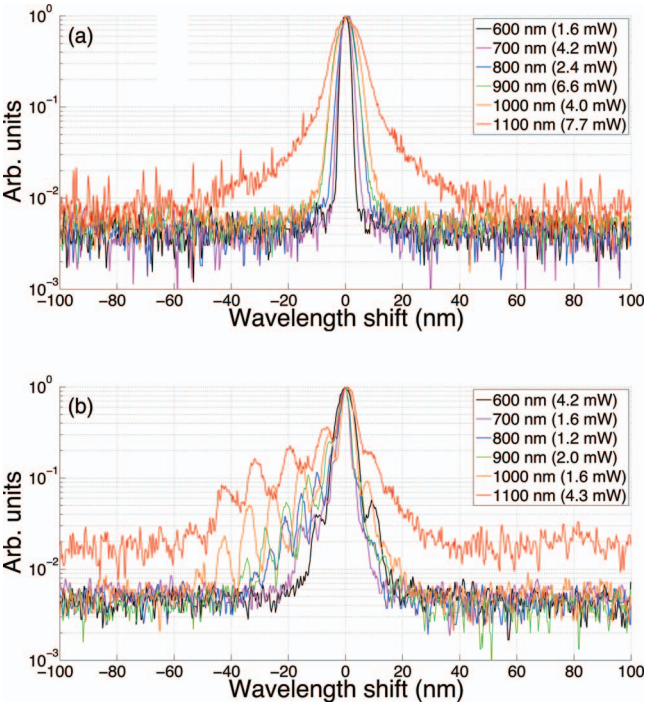

FIG. 2. Peak-normalized spectral response function at wavelengths ranging from 600 to 1100 nm for SYS1 (a) and SYS2 (b). The legend also reports the extracted power.

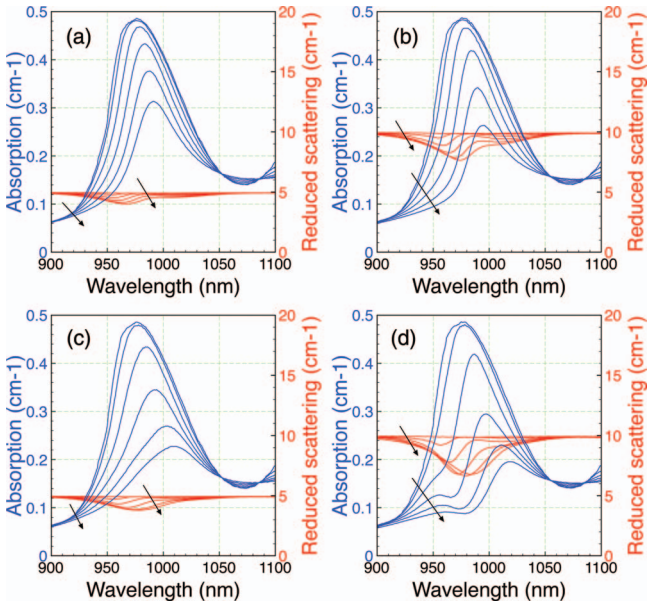

FIG. 3. Simulations of the water absorption peak for bandpasses ranging from 0 to 50 nm. Absorption and reduced scattering spectra are, respectively, represented in blue and red, respectively. (a) and (b) Simulations assume a bell-shaped gaussian SRF. (c) and (d) Simulations assume a sinc^2 SRF. (a) and (c) simulations are obtained with $\mu'_s = 5$ cm^{-1} and (b) and (d) with $\mu'_s = 10$ cm^{-1}.

respectively. The time-resolved curves obtained have been subsequently convolved with an experimental IRF and finally Poisson-noise has been added to better simulate measurement conditions. Finally, this dataset has been fitted with the same monochromatic theoretical model used for data generation using a Levenberg-Marquardt minimization procedure. The theoretical model is always convolved with the experimental IRF used to generate the dataset. Photons producing a signal lower than 80% and 10% of the peak, respectively, on the rising and trailing edge has been neglected. The results are shown in Fig. 3. Distortions in the absorption spectrum are stronger near the inflection point of both edges of the absorption spectrum, where the rate of variation is higher. Distortions due to the bandpass affect also the scattering spectrum, introducing deeps on the leading and falling edges of the spectrum. Distortions in both the absorption and scattering spectra are stronger on the simulations with higher μ'_s (Figs. 3(b)–3(d)). This is due to the fact that the cross talk between strongly and weakly absorbed photons depends exponentially on the photon TOF and for a higher μ'_s the mean photon TOF is longer. Distortions induced by a sinc^2 SRF (Figs. 3(c) and 3(d)) are stronger than those induced by a gaussian SRF (Figs. 3(a) and 3(b)). In particular, absorption and scattering spectra may show ripples due to the presence of side-lobes. These, in fact, enhance the contribution of low absorbed photon at wavelengths far from the nominal one. These photons cause a shallow slope of the TR curve that, after a certain time, overcomes the contribution due to photons at the nominal wavelength. Moreover, we observe a peak shift toward longer wavelengths due to the asymmetry of the absorption shape.

The observations discussed above have been confirmed by an experimental measurement. The sample consists of a 6.17% liquid solution of 20% calibrated Intralipid[16] in

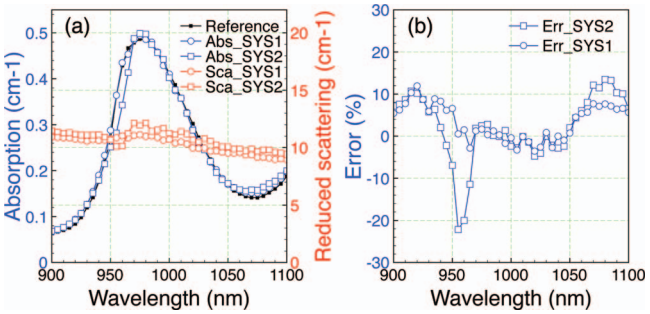

FIG. 4. (a) Water absorption (blue) and reduced scattering (red) spectra as measured by SYS1 (○) and SYS2 (□). (b) Relative error of the absorption spectrum measured with SYS1 (○) and SYS2 (□).

distilled water ($\mu'_s \sim 10$ cm^{-1}@900 nm) filling a 25 × 27 × 19 cm^3 black plastic tank. The sample was measured with SYS1 and SYS2 in reflectance geometry with 2 cm interfiber distance. The TOFs temporal distribution has been acquired in the spectral range 900–1100 nm in steps of 5 nm. The photon count-rate of the measure has been taken at about 800 Kcounts/s with a maximum acquisition time of 30 s. Data have been analyzed identically to the simulations: the diffuse reflectance at 2 cm source-detector separation for a semi-infinite medium has first been convolved with the IRF and then fitted to the experimental data for each wavelength. Retrieved absorption and scattering spectra, together with the relative error of the absorption spectrum, are shown, respectively, in Figs. 4(a) and 4(b). We observe that the absorption and reduced scattering spectra retrieved using SYS1 are slightly coupled near the peak wavelength. This effect, well known in the literature, is due to the low accuracy of the diffusion theory when the absorption is high.[15] By comparison with Fig. 3(b), the bandpass effect is clearly present in the spectrum deep above 1050 nm: the deep appears smoother than the one of the reference spectrum. On the contrary, the scattering spectrum at wavelengths longer than 1050 nm is not distorted, as confirmed by simulations. The spectrum retrieved by means of SYS2 instead shows stronger distortions with respect to the one retrieved using SYS1. Distortions are predominant on the rising edge of the absorption spectrum (producing error of about 20%) and a ripple on the scattering spectrum is also evident. Although the FWHM of the probing light of SYS2 is shorter than that of SYS1 for every wavelength longer than 900 nm, distortions induced by the AOTF are stronger. This indicates that the bandpass is not the only spectral parameter to control in designing a TRS system. Further, the prism-based approach offers greater flexibility in the spectral shaping of the beam. In fact, by properly adjusting the slit width (see Fig. 1) it is possible to gain power at the expenses of a broader bandpass if one needs a high power level for measurements.

In summary, this work has investigated and compared two approaches to the design of a system for TRS of diffusive media based on a supercontinuum source and based on a dispersive prism and on an AOTF, respectively. Power spectra measured after the wavelength selection stage show that with the first approach the extracted power is higher at the expense of a broader SRF at FWHM. With the second approach, one can obtain narrower SRF at FWHM but with a not negligible presence of side-lobes. The effects of the SRF of both systems on the estimated absorption and scattering spectra have then been investigated. Experimental results, confirmed also by numerical simulations, demonstrate that, notwithstanding the bandpass FWHM provided by the AOTF-based system is narrower than the one provided by the prism-based system, distortions induced by the former are stronger due to the presence of side-lobes. These distortions can dramatically affect the estimation of chromophore concentrations.

We wish to acknowledge partial support from the European Community's Seventh Framework Programme [FP7/2007-2013] under Grant Agreement No. 284464 (LASERLAB-EUROPE).

[1]B. J. Tromberg, N. Shah, R. Lanning, A. Cerussi, J. Espinoza, T. Pham, L. Svaasand, and J. Butler, Neoplasia **2**, 26 (2000).
[2]A. Bellincontro, A. Taticchi, M. Servili, S. Esposto, D. Farinelli, and F. Mencarelli, J. Agric. Food Chem. **60**, 2665 (2012).
[3]J. Johansson, S. Folestad, M. Josefson, A. Sparén, C. Abrahamsson, S. Andersson-Engels, S. Svanberg, and A. Sparen, Appl. Spectrosc. **56**, 725 (2002).
[4]C. D'Andrea, A. Farina, D. Comelli, A. Pifferi, P. Taroni, G. Valentini, R. Cubeddu, L. Zoia, M. Orlandi, and A. Kienle, Appl. Spectrosc. **62**, 569 (2008).
[5]R. M. P. Doornbos, R. Lang, M. C. Aalders, F. W. Cross, and H. J. C. M. Sterenborg, Phys. Med. Biol. **44**, 967 (1999).
[6]C. Abrahamsson, T. Svensson, S. Svanberg, S. Andersson-Engels, J. Johansson, and S. Folestad, Opt. Express **12**, 4103 (2004).
[7]A. Bassi, J. Swartling, C. D'Andrea, A. Pifferi, A. Torricelli, and R. Cubeddu, Opt. Lett. **29**, 2405 (2004).
[8]A. Pifferi, A. Torricelli, P. Taroni, D. Comelli, A. Bassi, and R. Cubeddu, Rev. Sci. Instrum. **78**, 053103 (2007).
[9]T. Svensson, E. Alerstam, D. Khoptyar, J. Johansson, S. Folestad, and S. Andersson-engels, Rev. Sci. Instrum. **80**, 063105 (2009).
[10]F. Bevilacqua, A. J. Berger, A. E. Cerussi, D. Jakubowski, and B. J. Tromberg, Appl. Opt. **39**, 6498 (2000).
[11]A. Bassi, A. Farina, C. D'Andrea, A. Pifferi, G. Valentini, and R. Cubeddu, Opt. Express **15**, 14482 (2007).
[12]M. Mazurenka, A. Jelzow, H. Wabnitz, D. Contini, L. Spinelli, A. Pifferi, R. Cubeddu, A. D. Mora, A. Tosi, F. Zappa, and R. Macdonald, Opt. Express **20**, 283 (2012).
[13]M. Bürmen, F. Pernuš, and B. Likar, Appl. Spectrosc. **65**, 393 (2011).
[14]A. Farina, A. Bassi, A. Pifferi, P. Taroni, D. Comelli, L. Spinelli, and R. Cubeddu, Appl. Spectrosc. **63**, 48 (2009).
[15]F. Martelli, S. Del Bianco, A. Ismaelli, and G. Zaccanti, *Light Propagation Through Biological Tissue and Other Diffusive Media* (SPIE, Bellingham, WA, 2010), p. 274.
[16]L. Spinelli, F. Martelli, A. Farina, A. Pifferi, A. Torricelli, R. Cubeddu, and G. Zaccanti, Opt. Express **15**, 6589 (2007).